J Mater Sci: Mater Med (2008) 19:2087–2096
DOI 10.1007/s10856-007-3293-1

Effect of thin carbonate-containing apatite (CA) coating of titanium fiber mesh on trabecular bone response

Tohru Hayakawa · Kenichi Takahashi · Hiroyuki Okada · Masao Yoshinari · Hiroki Hara · Chihiro Mochizuki · Hirotsugu Yamamoto · Mitsunobu Sato

Received: 10 May 2007 / Accepted: 25 September 2007 / Published online: 30 October 2007
© Springer Science+Business Media, LLC 2007

Abstract The influence of thin carbonate-containing apatite (CA) coating on trabecular bone response to cylindrical titanium fiber mesh (porosity of 85%, pore size of 200–300 μm, 2.8 mm diameter × 6 mm length) implants was investigated. Thin CA coatings were deposited by the so-called molecular precursor method. Molecular precursor solution was obtained by adding dibutylammonium diphosphate salt to Ca–EDTA/amine ethanol solution by adjusting Ca/P = 1.67. Sintered cylindrical titanium fiber mesh was immersed into molecular precursor solution and then tempered at 600 °C for 2 h. The immersion and tempering process was repeated three times. An adherent thin CA film could be deposited on the inside of titanium fiber mesh. After the immersion of a CA-coated titanium fiber mesh in simulated body fluid, apatite crystals precipitated on the titanium fiber mesh. Uncoated and CA-coated titanium fiber mesh was inserted into the trabecular bone of the left and right femoral condyles of rabbits. Histological and histomorphometrical evaluation revealed a significantly greater amount of bone formation inside the porous area of the CA-coated titanium fiber mesh after 12 weeks of implantation. The present results suggested that a thin CA-coated titanium mesh has better osteoconductivity and will be useful for a three-dimensional scaffold.

T. Hayakawa (✉) · K. Takahashi
Department of Dental Biomaterials, Nihon University School of Dentistry, 2-870-1, Sakaecho-nishi, Matsudo, Chiba 271-8587, Japan
e-mail: hayakawa.tohru@nihon-u.ac.jp

H. Okada · H. Yamamoto
Department of Oral Pathology, Nihon University School of Dentistry, 2-870-1, Sakaecho-nishi, Matsudo, Chiba 271-8587, Japan

M. Yoshinari
Department of Dental Materials Science and Oral Health Science Center, Tokyo Dental College, 1-2-2 Masago, Mihamaku, Chiba 261-8502, Japan

H. Hara · C. Mochizuki · M. Sato
Coordination Engineering Laboratory, Faculty of Engineering, Kogakuin University, 2665-1, Nakano, Hachioji, Tokyo 192-0015, Japan

1 Introduction

Currently, biocompatible ceramics or biodegradable polymers are widely used as a scaffold or carrier material for bone graft substitutes [1–3]. In particular, porous materials are beneficial for a scaffold because of the migration or proliferation of cells, in growth of living tissues into the pores and long-term stability by mechanical interlocking; however, these materials have the disadvantage of insufficient mechanical properties, brittleness or easy transformation [4, 5]. Another candidate porous scaffold material for bone graft substitutes is titanium fiber mesh [6], which is non-degradable three-dimensional scaffold material. Titanium fiber mesh has sufficient stiffness and elasticity, and it is bone compatible and easy to handle during surgery. Pioneering and valuable studies of titanium fiber mesh as a scaffold material have been performed by Jansen et al. [7–11]. They loaded bone marrow stromal cells or growth factor on titanium fiber mesh and demonstrated the efficacy of titanium fiber mesh as a scaffold material.

Vehof et al. [12] tried to deposit a thin calcium phosphate coating on titanium fiber mesh using the RF magnetron sputtering technique [13], which is a

representative physical vapor deposition technique, and evaluated bone formation either without or loaded with cultured rat bone marrow cells by subcutaneous implantation into the back of rats. In this article they described that thin RF magnetron sputter coating did not penetrate completely throughout the mesh so the inside of the mesh still consisted of the original titanium; as a result, the absence of bonding osteogenesis was due to insufficient deposition of calcium phosphate coating of titanium fiber mesh. Tsukeoka et al. [14] incorporated hydroxyapatite particles in titanium fiber mesh by the dipping technique, and found that hydroxyapatite-incorporated titanium fiber mesh showed higher bonding strength to the femur of dogs and larger bone in growth deep inside titanium fiber mesh in the initial stage after operation. On the basis of the above results, it is speculated that the effective deposition of Ca–P coating onto or inside titanium fiber mesh will produce better bone response.

Recently, Sato et al. [15] found that carbonate-containing apatite (CA) can be deposited on titanium by using a precursor solution containing a Ca–EDTA complex and phosphate compounds, called the molecular precursor method. Takahashi et al. [16] reported that tempering at 600 or 700 °C formed crystalline CA films on titanium substrates with the molecular precursor method. In a very simple procedure, they dropped the molecular precursor solution on the titanium substrate and then tempered. The film thickness was less than 1 μm, and the tensile bond strength measurement and scratch test showed an excellent degree of adhesion of the coated film on titanium after immersion in phosphate-buffered saline (PBS, pH 7.4) solution. Moreover, a greater precipitation of calcium phosphate crystals was observed on the titanium plate coated with a CA thin film after immersion in simulated body fluid (SBF) compared with an uncoated titanium plate surface [17]. In vivo animal experiments demonstrated that titanium cylindrical implants coated with CA film showed greater bone-to-implant contact during the healing phase than uncoated titanium [18].

The molecular precursor method is a wet process. Our previous study revealed that CA thin film could be deposited not only on the surface but also on the inside of titanium fiber mesh by immersion in molecular precursor solution [19].

In the present study, we aimed to evaluate the biological response of titanium fiber mesh coated with CA thin film using the molecular precursor method. The bone response inside the titanium fiber mesh coated with CA thin film was compared with unaltered control titanium fiber mesh after implantation into the trabecular bone of the femoral condyles of rabbits.

2 Materials and methods

2.1 Preparation of molecular precursor solution

The molecular precursor solution for the CA coating was prepared by adding dibutylammonium diphosphate salt to a Ca–EDTA/amine ethanol solution. The general procedure for the preparation of the molecular precursor solution is shown in Fig. 1, according to previous articles [16–19].

The molecular precursor solution was prepared in three steps. During step 1, Ca–EDTA/amine ethanol solution was prepared from the reaction of $CaH_2(edta) \cdot 2H_2O$ and dibutylamine ethanol under reflux conditions. $CaH_2(edta) \cdot 2H_2O$ was obtained from the reaction of EDTA and

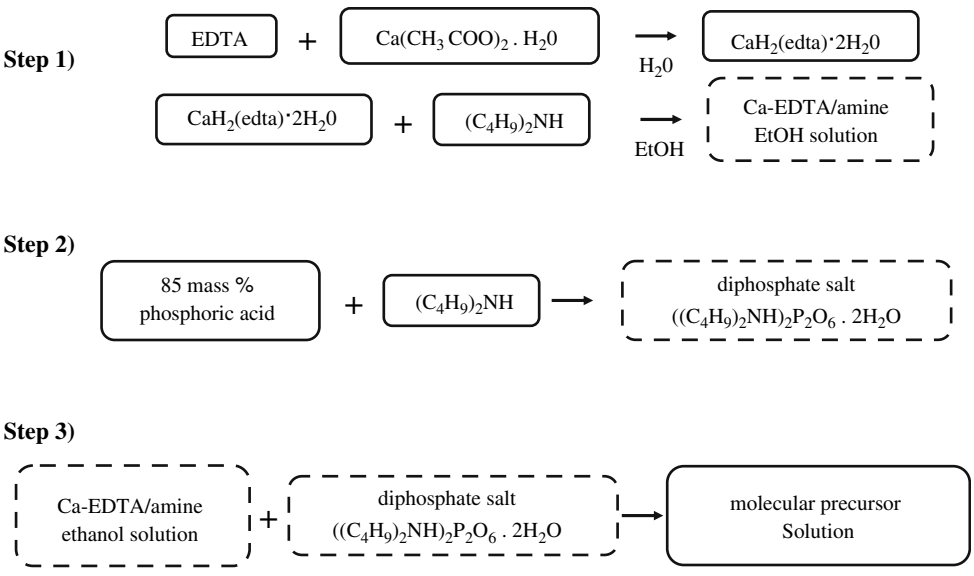

Fig. 1 Schematic presentation of the preparation of the molecular precursor solution

$Ca(CH_3COOH)_2$. A clear Ca–EDTA/amine ethanol solution was obtained. During step 2, dibutylammonium diphosphate salt ($((C_4H_9)_2NH_2)_2P_2O_6 \cdot 2H_2O$) was obtained as a white precipitate from the reaction of 85% mass phosphoric acid and an ethanol solution of dibutylamine. Finally step 3, the molecular precursor solution was obtained by adding dibutylammonium diphosphate salt to the Ca–EDTA/amine ethanol solution by adjusting Ca/P = 1.67.

2.2 Titanium fiber mesh

Sintered cylindrical titanium fiber mesh (Fig. 2, Bekinit, Tokyo, Japan) with a volumetric porosity of 85%, weight of 3,400 g/m^2, was used. The prepared implants were cylindrical with a diameter of 2.8 mm and length of 6 mm. Titanium fiber mesh is fabricated by interengaging and intertwining a multiplicity of thin titanium fibers. The fibers are bonded at their points of contact using a sinter process. This results in very open interconnected porosity.

The surface of titanium fiber mesh was observed by field-emission scanning electron microscope (FE-SEM, JSM-6340F, JEOL, Tokyo, Japan) at an accelerating voltage of 5 kV.

Twenty-four cylindrical sintered titanium fiber mesh implants were used. Half of the implants were left uncoated and the other half was given a thin CA coating using the molecular precursor method.

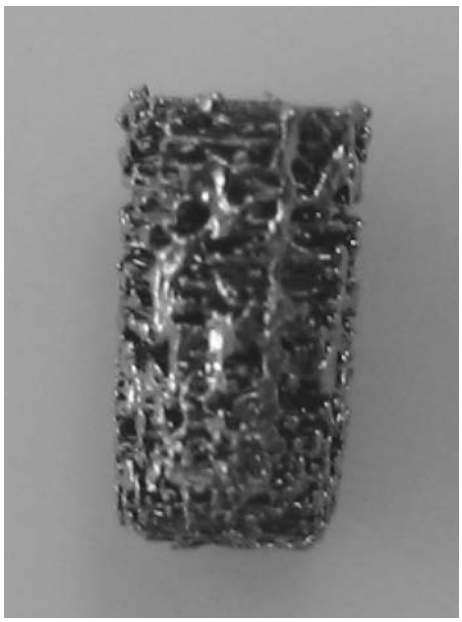

Fig. 2 Titanium fiber mesh used in the present study (diameter 2.8 mm, length 6 mm)

2.3 CA coating

The coating procedure was performed according to the previously described method [16–19]. Before coating, titanium implants were cleaned ultrasonically in propanol, and then dried at 100 °C. The implants were immersed in molecular precursor solution for 20 min with ultrasonic treatment. Ultrasonic treatment improved the penetration of precursor solution into the titanium fiber mesh. Subsequently, the precursor films that formed on the titanium cylinder were dried at 60 °C for 20 min and then tempered at 600 °C for 2 h using a furnace (MSFT-1520-P, Nikkato, Tokyo, Japan) under atmospheric conditions. The immersion of the titanium fiber mesh implant in molecular precursor solution and tempering at 600 °C process was repeated three times.

The effectiveness of coating of CA film inside titanium fiber mesh was evaluated using EPMA (JXA-8200, JEOL, Tokyo, Japan) at an accelerating voltage of 25 kV by detecting the X-ray intensity of Ca-Kα, P-Kα, and Ti-Kα. The specimens were embedded in epoxy resin. After curing the resin, the specimens were cut in the middle of the specimens using a cutting machine (Finecut, HS-100, Heiwa Tech, Japan) to observe the inside of the titanium fiber mesh. These specimens were grounded down to 1,200 grit with abrasive papers, polished using 0.3 μm alumina, and then ultrasonically cleaned with ethanol and distilled water. Afterwards, carbon was coated on the specimens before EPMA analysis. The presence of CA coating inside the titanium mesh was confirmed by the elementary mapping of calcium, phosphorous, and titanium.

The deposited CA layer was also characterized by micro-X-ray diffraction (micro-XRD, θ–2θ diffractometer, D8 Discover with Gadds, Bruker Axs, Kanagawa, Japan), which had an X-ray source of Cu-Kα, and a power of 45 kV × 110 mA. It is possible to measure very thin and complicated CA coating using the micro-XRD technique. Twenty-two points of coated cylindrical titanium fiber mesh were measured by 0.1 mm step in the *y*-axis direction.

After coating, the implants were cleaned ultrasonically in acetone, boiled in ethanol and dried.

2.4 Immersion in simulated body fluid

As in vitro biocompatibility evaluation, the influence of a thin CA coating was checked by monitoring apatite formation in SBF. Uncoated and CA-coated titanium cylinders were immersed in 20 mL of SBF, Hanks' balanced salt solution (HBSS) without organic species (pH = 7.4) [20, 21], at 37 °C in sealed polystyrene bottles for 14 days. The ion concentrations of HBSS are listed in Table 1. The solutions and bottles were changed every day

Table 1 Bone ingrowth percentage into the space of titanium fiber mesh

Uncoated	CA-coated
3.3 ± 1.6	30.5 ± 16.7

Mean ± SD. Significant difference between mean values existed ($p < 0.05$)

to expose the specimens to fresh solutions. After immersion, the titanium fiber mesh was rinsed with double-distilled water to remove HBSS solution, and then dried in a desiccator. The surface of the samples was examined by FE-SEM at an accelerating voltage of 5 kV, and the crystallographic structure of precipitates on titanium fiber mesh was analyzed by X-ray diffraction (RINT2000, Rigaku, Tokyo, Japan), which had an X-ray source of Cu-Kα and a power of 50 kV × 100 mA.

2.5 Implantation procedure

The animal study was conducted in accordance with the animal experimental ethical guidelines of Nihon University School of Dentistry at Matsudo (Certificate Number: ECA-05-0016). Eight 3-month-old female Japanese White Rabbits weighing about 3.5–4 kg were used.

The implants were inserted into the trabecular bone of rabbits according to a previously used technique [13, 18]. Each animal received two implants: one in the left and one in the right medial femoral condyle. A total of 16 titanium fiber mesh implants were placed: eight uncoated, eight CA-coated. Before surgery, all implants were sterilized in an autoclave.

Surgery was performed under general inhalation anesthesia with a 4% isoflurane and oxygen mixture which was reduced to 2% isoflurane during surgical manipulation. Local anesthesia was performed by injection of xylocain. To reduce the preoperative infection risk, a prophylactic antibiotic, Shiomalin® (equivalent to Latamoxef Sodium), was administered postoperatively by subcutaneous injection. The titanium fiber mesh implants were inserted into the left and right medial femoral condyles of the rabbits. For insertion of the titanium fiber mesh, each animal was immobilized on its back. The hind legs of the rabbits were shaved, washed and disinfected with iodine tincture.

A longitudinal incision was made on the medial surface of the left and right femur, and the medial condyle was exposed. After exposure of the femoral condyle, a pilot hole, 0.6 mm, was drilled. The hole was gradually widened with different drills to the final diameter (2.8 mm) of the implant. The bone was prepared with a very gentle surgical technique using a low rotational drilling speed (500 rpm) and continuous internal cooling. After press-fit insertion of the implants, the soft tissues were closed in separate layers using restorable Vicryl 3–0 sutures.

Finally, the position and fit of the titanium fiber mesh were confirmed radiographically. The titanium fiber mesh implants were placed transversely across the femoral condyle. Only at the cortical side, the implants were surrounded by cortical bone. For the rest, the implants were fully placed in trabecular bone.

Postoperatively, the animals were placed in a standard cage. They were fed with water and rabbit diet ad libitum, and were allowed to move unrestricted at all times. The rabbits were killed by injecting an overdose of pentobarbital sodium (Nembutal®) peritoneally, according to the following scheme: four rabbits after 3 weeks of implantation, and four after 12 weeks ($n = 4$ for each material and implantation).

2.6 Histological procedures and evaluation

The implants and surrounding bone were excised immediately after sacrifice. Then, excess tissue of the excised femurs was removed. Following fixation in 10% buffered formalin solution, the specimens were prepared for histological evaluation. Implants containing tissue blocks were dehydrated through a graded series of ethanol and embedded in methylmethacrylate. After polymerization, non-decalcified thin sections were prepared using a cutting-grinding technique (EXAKT-Cutting Grinding System, BS-300CP band system and 400 CS micro grinding system, EXAKT) [22]. Sections were made in a transverse direction perpendicular to the axis of the implants, and were stained with methylene blue and basic fuchsin. The bone formation inside the titanium fiber mesh was evaluated using a light microscope (Eclipse E800M, Nikon, magnification 100×).

Besides a descriptive evaluation, the bone ingrowth ratio into titanium fiber mesh was determined for 12 week specimens. The amount of bone mass inside the titanium fiber mesh was measured and the rate of bone ingrowth area was defined as the percentage of bone mass to the porous area available for bone ingrowth inside the titanium fiber mesh. Four or five sections were prepared from the same titanium fiber mesh implant and one or two sections were used for histomorphometrical evaluation. All measurements were performed on sections taken from the middle part of the fiber mesh implant. This part was completely surrounded by trabecular bone. The measurements were made using a light microscope (Eclipse E800M, Nikon, magnification 12.5–125×) connected to a computer equipped with a video camera (KY-F55B, Victor, Yokohama, Japan) and an image analysis system (Image-Pro Plus, Media Cybernetics, Silver Spring, MD, USA). All

measurements were statistically evaluated using one-way ANOVA and Fisher's test for multiple comparison among the means at $p = 0.05$.

3 Results

3.1 CA coating

From the FE-SEM observation shown in Fig. 3, the surface of the fiber structure was clear identified and the average pore size was approximately 200–300 μm.

An SEM image of the cross section of titanium fiber mesh, used for EPMA analysis, is shown in Fig. 4. Two boxed areas, the surface and inside center of titanium fiber mesh, were analyzed. It revealed that the inside area of titanium fiber mesh also has an average pore size of approximately 200–300 μm. Figures 5 and 6 show the elementary distribution of titanium fiber mesh after CA coating. The elementary distribution of P, Ca, Ti is demonstrated together with the SEM image of titanium fibers (SL). Mapping of Ti showed the titanium fiber structure. It found that P and Ca are present not only along with the surface area of titanium fiber mesh (Fig. 4) but also the inside center of titanium fiber mesh (Fig. 5). The results supported that thin CA film could cover the inside center area as well as the surface of titanium fiber mesh using molecular precursor solution.

Figure 7 shows the XRD patterns after coating titanium fiber mesh. The XRD pattern showed that the deposit coating had apatite structures by a reflection peak around $2\theta = 26°$ (002), and 32–33 (211, 112, 300). The reflection of the rutile peak resulted from the heat treatment of titanium fiber mesh.

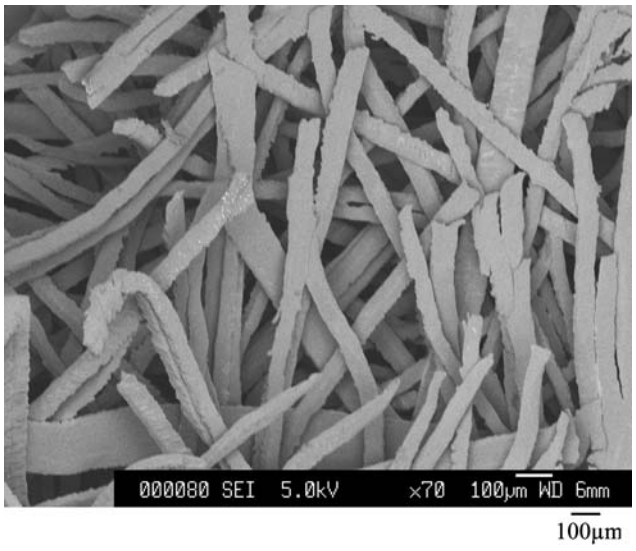

Fig. 3 FE-SEM picture of Ti fiber mesh. The surface of the fiber structure was clearly identified. Average pore size was approximately 200–300 μm. (bar = 100 μm)

Fig. 4 SEM image of cross section of titanium fiber mesh for EPMA analysis. Two boxed areas, surface and inside center of Ti fiber mesh, were analyzed. The inside area of titanium fiber mesh also had an average pore size of approximately 200–300 μm. (bar = 100 μm)

3.2 Immersion in simulated body fluid

After immersion in HBSS for 14 days, the formation of white precipitated on CA-coated titanium fiber was observed, whereas no precipitation was observed on uncoated titanium fibers during the same immersion period.

Figure 8 shows a FE-SEM picture of the surface of titanium fiber mesh implant after immersion in HBSS. Scanning electron microscopic observation revealed that each fiber was completely covered with white precipitates.

Figure 9 shows XRD patterns of white precipitates on titanium fiber mesh. Major peaks in the spectrum could be assigned as 002, 211, 112, 300, 310, 222, and 213 peaks of hydroxyapatite.

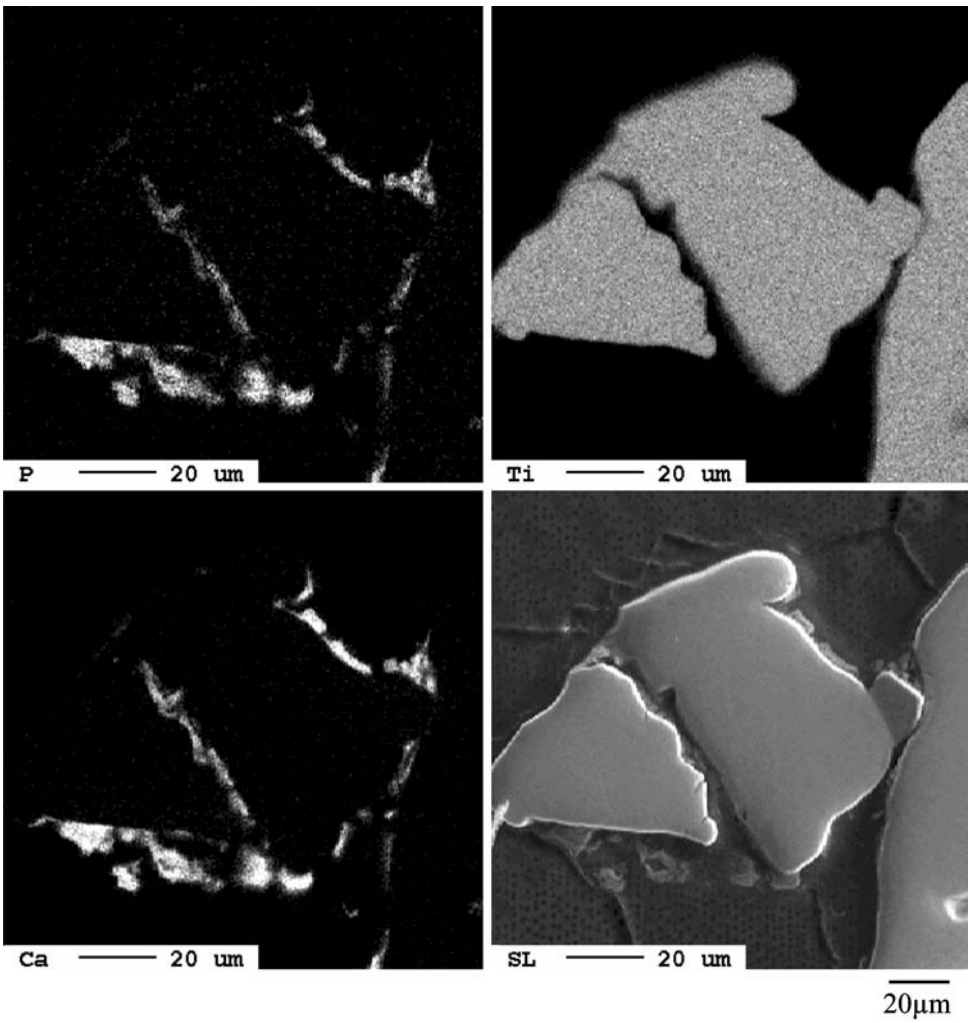

Fig. 5 EPMA analyses of the surface area of Ti fiber mesh. Mapping of Ti showed the titanium fiber structure. P and Ca are present along with the surface area of Ti fiber mesh. (bar = 20 μm)

3.3 Histology and histomorphometrical evaluation

During the test periods, the experimental animals remained in good health. At sacrifice, no clinical signs of inflammation or adverse tissue reactions were seen. All titanium fiber mesh implants were still in situ at sacrifice.

The overall trabecular bone response to the two different implant surfaces at 3 weeks after implantation was similar to that shown in Fig. 10. Clear signs of primary woven bone formation were observed. Only a few bones were present in the space of titanium fiber mesh. The presence of lacunae was observed. In addition, small bone fragments could be observed, which were apparently loosened during the drilling process. The bone fragments were interspersed between the bone marrow spaces.

At 12 weeks, bone remodeling was completed and the new bone had completely remodeled into mature trabecular bone. Thicker bone formation was recognized. The bone response to different titanium fiber mesh was clearly different, as shown in Fig. 11. More bone ingrowth was observed in the space of CA-coated titanium fiber mesh. Most of the new bone formation was not recognized with uncoated titanium fiber mesh.

Table 1 shows the results of the measured percentage of bone ingrowth into the space of titanium fiber mesh. CA-coated titanium fiber mesh provided significantly higher bone ingrowth into the space compared with uncoated titanium fiber mesh ($p < 0.05$).

4 Discussion

The aim of the present study was to evaluate the effect of a CA coating for titanium fiber mesh on the trabecular bone response.

Our previous animal study revealed that an adherent thin CA film deposited using the molecular precursor method on cylindrical titanium implants showed greater bone-to-implant contact during the healing phase than uncoated titanium implants [19]. In the present study, a thin CA

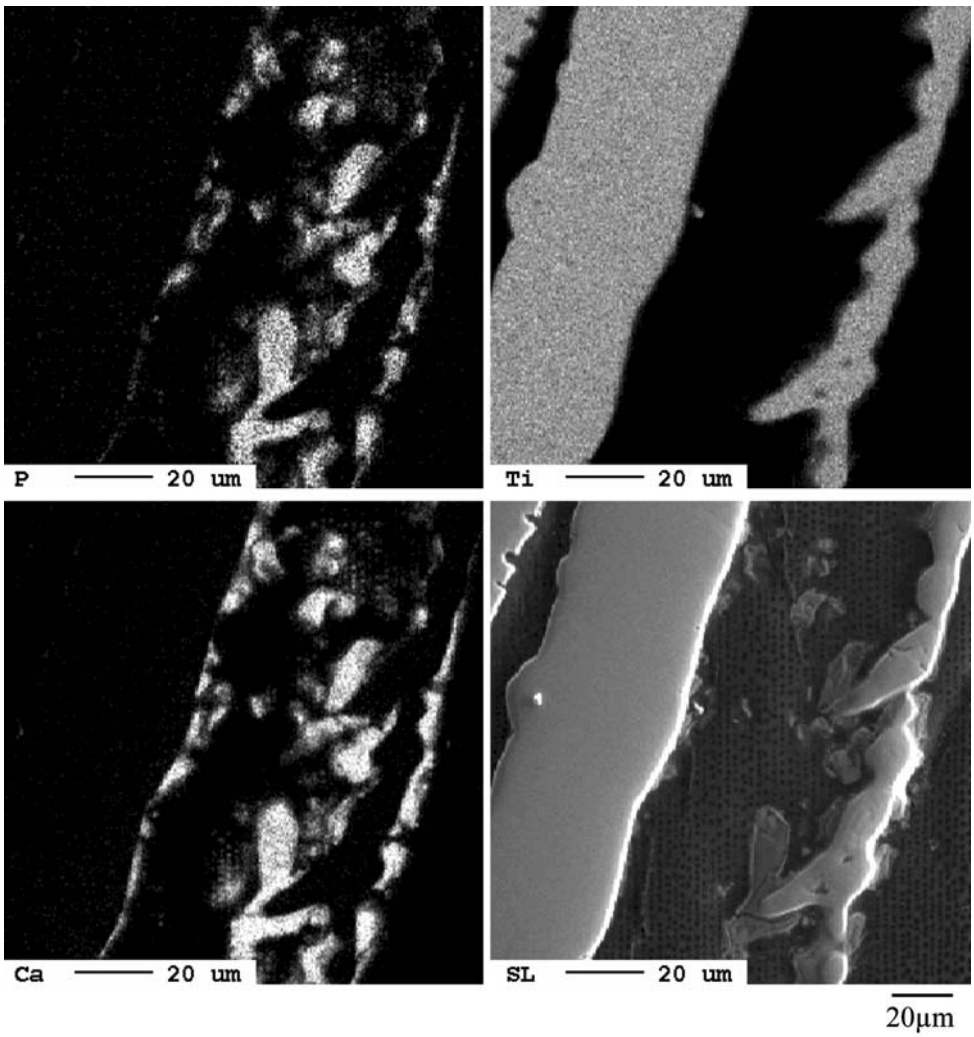

Fig. 6 EPMA analyses of the inside center area of Ti fiber mesh. Mapping of Ti showed the Ti fiber structure. P and Ca are present inside the center of Ti fiber mesh. (bar = 20 μm)

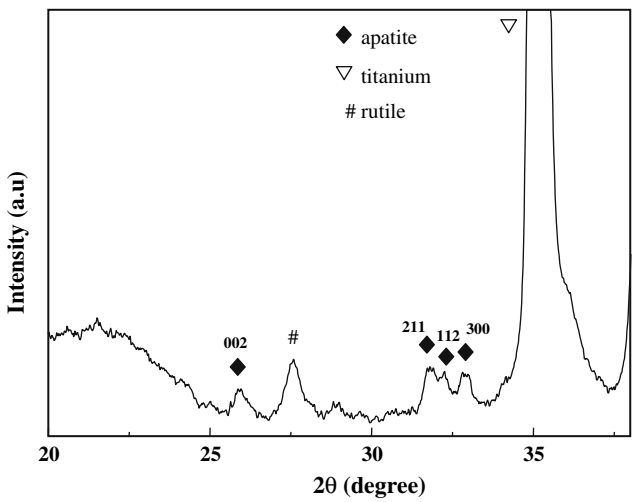

Fig. 7 X-ray diffraction pattern of apatite-coated Ti fiber mesh. Apatite structure was identified

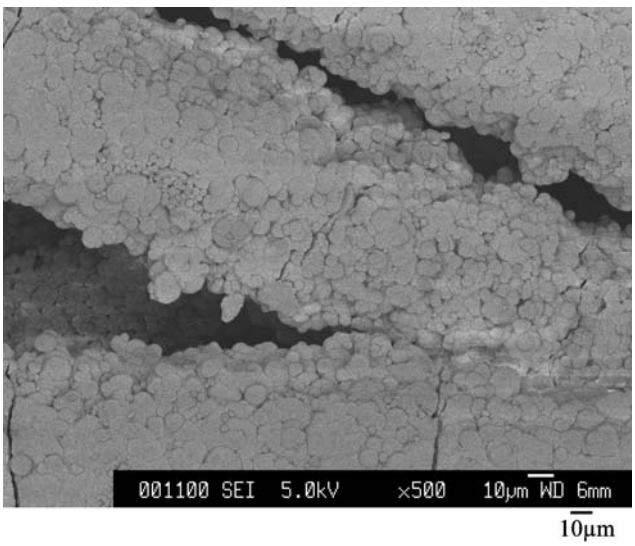

Fig. 8 FE-SEM picture of apatite precipitates on a CA-coated Ti fiber mesh after immersion in HBSS. Titanium fibers were completely covered with apatite crystals. (bar = 10 μm)

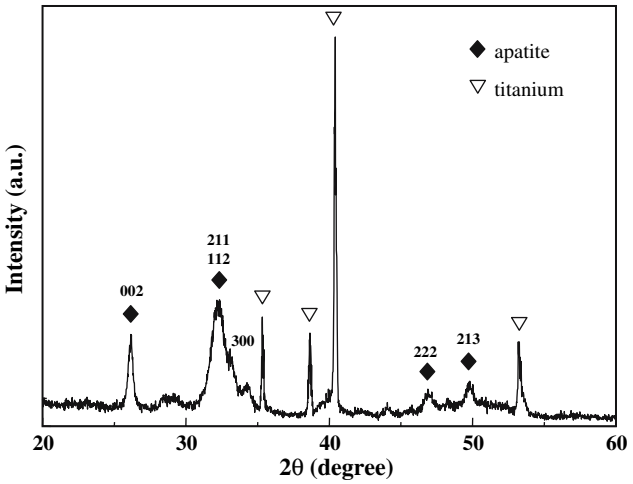

Fig. 9 X-ray diffraction pattern of apatite precipitates on CA-coated Ti fiber mesh after immersion in HBSS

coating was applied to titanium fiber mesh, and better bone response was also obtained by a thin CA coating using the molecular precursor method.

The advantage of the molecular precursor method is that CA coating can be deposited onto titanium implants of any shape. Moreover, the deposited thin film produced by the molecular precursor method already possesses a crystalline structure, which avoids the use of post-deposition annealing procedures. For example, PVD methods provide amorphous Ca–P coatings, and heat treatment procedures are needed to obtain crystalline apatitic film [23]. Namely, two steps, the deposition of apatitic film and heat treatment crystallization is needed for PVD methods, while when using molecular precursor methods, crystalline apatitic film can be deposited in one-step for coating titanium disk or cylinder. Another advantage of the molecular precursor method is that control of the Ca/P ratio is very easy by changing the mixing ratio of dibutylammonium diphosphate salt and Ca–EDTA/amine ethanol solution. Further study will elucidate the possibility of depositing calcium phosphate film with different Ca/P ratios, such as tricalcium phosphate film, using the molecular precursor method.

CA coating could be possible for titanium fiber mesh using molecular precursor method. But one-time application of the molecular precursor process, immersion into molecular precursor solution and tempering, to titanium fiber mesh was insufficient. The inside area of titanium fiber mesh could not be effectively coated due to insufficient penetration of the molecular precursor solution into the titanium fiber mesh. It was previously demonstrated that three-time application of the molecular precursor process was effective for coating titanium fiber mesh with a disk shape, not only the surface area but also inside [19]. Our present study also demonstrated that three-time application of the molecular precursor process was effective for coating cylindrical titanium fiber mesh.

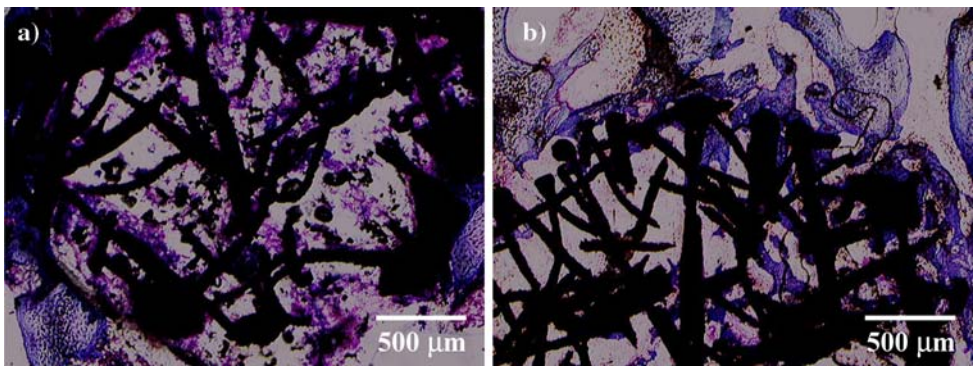

Fig. 10 Histological appearance of Ti fiber mesh after 3 weeks of implantation. Only a few bones are present in the space of uncoated and CA-coated Ti fiber mesh. (**a**) uncoated Ti fiber mesh and (**b**) thin CA-coated Ti fiber mesh (Original magnification 85×, bar = 500 μm)

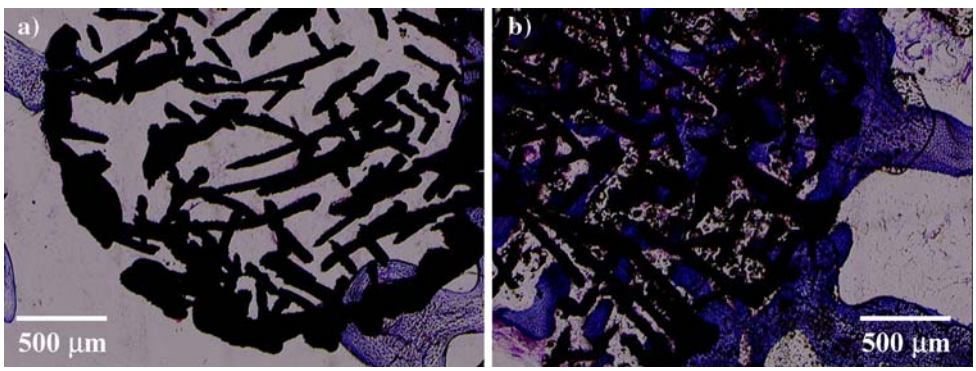

Fig. 11 Histological appearance of Ti fiber mesh after 12 weeks of implantation. More bone ingrowth was observed in the spaces of CA-coated Ti fiber mesh. (**a**) Uncoated Ti fiber mesh. (**b**) Thin CA-coated Ti fiber mesh (Original magnification85×, bar = 500 μm)

A biomimetic process using simulated body fluid for apatite coating has been proposed [24, 25]. Apatite crystals were deposited onto the titanium surface in simulated body fluid. This process also enables the deposition of hydroxyapatite onto any shape of substrate. Fujibayashi et al. [26] and Takemoto et al. [27] deposited apatite crystals on the whole surface of porous bioacitive titanium mesh (porosity of 40–60%); however, in this process, titanium should be treated by NaOH and heated before immersion in simulated body fluid and it took at least several days to form a hydroxyapatite layer on titanium. On the other hand, there is no need for pretreatment of the titanium surface using the molecular precursor method and it took only a few hours for apatite deposition.

For the evaluation of in vitro biocompatibility, many studies have reported the formation of an apatite layer after materials are immersed in SBF. It is reported that in vivo bioactivity (osteoconductivity) of biomaterials such as ceramics is precisely mirrored by their in vitro apatite-forming ability in an SBF [28]. In the present study, HBSS was employed as SBF. Hanawa et al. [21] reported that an apatite layer was formed on the titanium surface after immersion in HBSS. Tanimoto et al. [29] reported that in vivo bone formation of sintered tricalcium sheets confirmed the results of the in vitro SBF immersion experiment, namely more apatite formation corresponded with better bone formation.

At 3 weeks of implantation, primary woven bone formation hampered the correct quantification of bone reaction. Quantification analysis for bone ingrowth was performed only at 12 weeks. Our present in vitro apatite formation in SBF result corresponded with in vivo bone formation. Apatite formation after HBSS immersion and more bone formation inside titanium fiber mesh were observed for a thin CA-coated titanium fiber mesh. This was due to the improvement of osteoconductivity by a thin CA coating.

Previous studies revealed that crystalline thin CA films produced by the molecular precursor method were stable after 12-month immersion in PBS solution, and it is also claimed that a slight decrease of the Ca/P ratio of the coating was observed after PBS immersion [17]. It was assumed that an ion exchange reaction between coated film and PBS solution partly occurred via the dissolution/precipitation process. The in vivo dissolution behavior of the present CA films remains unclear. In general, we have to be aware that an adequate insight into the role of CA coating in bone healing is still lacking.

The pore size and porosity of titanium fiber mesh used in the present study was based on the reports of Jansen and colleagues [6–12]. The present titanium fiber mesh has a porosity of 85%, which is greater than those of fiber mesh (porosity of 40–60%) by Fujibayashi et al. [26] and Takemoto et al. [27]. It is presumed that a higher porosity of titanium fiber mesh will induce better tissue integration and provide fewer mechanical properties. Analysis of the mechanical properties of the present fiber mesh titanium (porosity of 85%) will be further investigated.

We could produce a sufficiently CA-coated titanium fiber mesh by molecular precursor method. CA-coated titanium fiber mesh will be used as a bone substitute and will also be useful for loading cytokines such as BMP or other biological molecules. Yoshinari et al. [30] reported that bisphosphonate, which is a drug used to treat osteoporosis, exhibited better binding to apatite-coated titanium compared to uncoated titanium. They also reported that a thin coating of calcium phosphate followed by bisphosphonate immobilization is effective in the promotion of osteogenesis on the surfaces of dental implants [31].

In conclusion, thin CA-coated titanium fiber mesh produced using the molecular precursor method enhanced bone ingrowth. It is suggested that thin CA-coated titanium fiber mesh will be a good candidate for a three-dimensional scaffold for regenerative medicine.

Acknowledgments This study was supported in part by a Grant-in-Aid for Scientific Research (C)(19592260) from the Japan Society for the Promotion of Science and by Oral Health Science Center Grant HRC7 from Tokyo Dental College, and by the Laboratory for Electron Beam Research and Application (LEBRA), Nihon University.

References

1. U. A. STOCK and J. E. MAYER, *J. Long. Term. Eff. Med. Implants.* **11** (2001) 249
2. Y. TIELIEWUHAN, I. HIRATA, A. SASAKI, H. MINAGI and M. OKAZAKI, *Dent. Mater. J.* **23** (2004) 258
3. V. KAQRAGEORGIOU and D. KAPLAN, *Biomaterials* **26** (2005) 5474
4. R. ZHANG and P. X. MA, *J. Biomed. Mater. Res.* **44** (1999) 446
5. T. S. GIRTON, T. R. OEGEMA and R. T. TRANQUILLO, *J. Biomed. Mater. Res.* **46** (1999) 87
6. J. A. JANSEN, A. F. von RECUM, J. P. C. M. van der WAERDEN and K. de GROOT, *Biomaterials* **13** (1992) 959
7. J. W. M. VEHOF, A. D. de RUIJTER, P. H. M. SPAUWEN and J. A. JANSEN, *Tissue Eng.* **7** (2001) 373
8. E. H. M. HARTMAN, J. W. M. VEHOF, J. E. de RUIJTER, P. H. M. SPAUWEN and J. A. JANSEN, *Biomaterials* **25** (2004) 5831
9. J. A. JANSEN, J. W. M. VEHOF, P. Q. RUHE, H. KROEZE-DEUTMAN Y. KUBOKI, H. TAKITA, E. L. HEDBERG and A. G. MIKOS, *J. Controll. Release* **101** (2005) 127
10. H. L. HOLTORF, J. A. JANSEN and A. G. MIKS, *J. Biomed. Mater. Res.* **72A** (2005) 326
11. X. F. WALBOOMERS, S. E. ELDER, J. D. BUMGARDNER and J. A. JANSEN, *J. Biomed. Mater. Res.* **76A** (2006) 16
12. J. W. M. VEHOF, P. H. M. SPAUWEN and J. A. JANSEN, *Biomaterials* **21** (2000) 2003
13. T. HAYAKAWA, M. YOSHINARI, K. NEMOTO, J. G. C. WOLKE and J. A. JANSEN, *Clin. Oral Impl. Res.* **11** (2000) 296
14. T. TSUKEOKA, M. SUZUKI, C. OHTSUKI, Y. TSUNEIZUMI, J. MIYAGI, A. SUGINO, T. INOUE, R. MICHIHIRO and H. MORIYA, *J. Biomed. Mater. Res.* **75B** (2005) 168

15. M. SATO, C. MOCHIZUKI and K. YAMADA, in Proceedings of 6th International Porphyrin-Heme Symposium in Association with 9th International SPACC Symposium. Tokyo, Japan, 2002, edited by Ichiro Okura (ISSN:0918-4368) p. 97
16. K. TAKAHASHI, T. HAYAKAWA, M. YOSHINARI, H. HARA, C. MOCHIZUKI, M. SATO and K. NEMOTO, *Thin Solid Films* **484** (2005) 1
17. K. TAKAHASHI, T. HAYAKAWA, H. HARA, M. YOSHINARI, C. MOCHIZUKI, M. SATO, K. NEMOTO, *J. J. Dent. Mater.* **24** (2005) 39
18. T. HAYAKAWA, K. TAKAHASHI, M. YOSHINARI, H. OKADA, H. YAMAMOTO, M. SATO and K. NEMOTO, *Int. J. Oral Maxillofac. Implants* **21** (2006) 851
19. T. HAYAKAWA, K. TAKAHASHI, M. YOSHINARI, H. HARA, K. NEMOTO and M. SATO, *J. Oral Tissue Eng.* **3** (2005) 17
20. T. HANAWA, M. KON, H. UKAI, K. MURAKAMI, Y. MIYAMOTO and K. ASAOKA, *J. Biomed. Mater. Res.* **34** (1997) 273
21. T. HANAWA and M. OHTA, *Bioamterials* **12** (1991) 767
22. K. DONATH and G. A. BREUNER, *J. Oral Pathol.* **11** (1982) 318
23. M. YOSHINARI, T. HAYAKAWA, J. G. C. WOLKE, K. NEMOTO and J. A. JANSEN, *J. Biomed. Mater. Res.* **37** (1997) 60
24. H. TAKADAMA, H. M. KIM, T. KOKUBO and T. NAKAMURA, *J. Biomed. Mater. Res.* **27** (2001) 441
25. H. M. KIM, T. HIMENO, M. KAWASHITA, J. H. LEE, T. KOKUBO and T. NAKAMURA, *J. Biomed. Mater. Res.* **67** (2003) 1305
26. S. FUJIBAYASHI, M. NEO, H. M. KIM, T. KOKUBO and T. NAKAMURA, *Biomaterials* **25** (2004) 443
27. M. TAKEMOTO, S. FUJIBAYASHI, M. NEO, J. SUZUKI, Y. KOKUBO and T. NAKAMURA, *Biomaterials* **26** (2005) 6014
28. S. FUJIBAYASHI, M. NEO, H. M. KIM, T. KOKUBO and T. NAKAMURA, *Biomaterials* **24** (2003) 1349
29. Y. TANIMOTO, T. HAYAKAWA, T. SAKE and K. NEMOTO, *J. Biomed. Mater. Res.* **76A** (2006) 571
30. M. YOSHINARI, Y. ODA, H. UEKI and S. YOKOSE, *Biomaterials* **22** (2001) 709
31. M. YOSHINARI, Y. ODA, T. INOUE, K. MATSUZAKA and M. SHIMONO, *Biomaterials* **23** (2002) 2879